Measurement of Cerebral Glucose Metabolic Rates in the Anesthetized Rat by Dynamic Scanning with ^{18}F-FDG, the ATLAS Small Animal PET Scanner, and Arterial Blood Sampling

Kazuaki Shimoji, MD[1]; Laura Ravasi, MD[1,2]; Kathleen Schmidt, MA[3]; Maria Luisa Soto-Montenegro, PhD[4]; Takanori Esaki, MD[3]; Jurgen Seidel, PhD[5]; Elaine Jagoda, MS[1]; Louis Sokoloff, MD[3]; Michael V. Green, MS[5]; and William C. Eckelman, PhD[1]

[1]Positron Emission Tomography Department, Clinical Center, National Institutes of Health, Bethesda, Maryland; [2]Istituto di Scienze Radiologiche, Università degli Studi di Milano, Milano, Italy; [3]Laboratory of Cerebral Metabolism, National Institute of Mental Health, Bethesda, Maryland; [4]Hospital General Universitario Gregorio Marañón, Madrid, Spain; and [5]Department of Nuclear Medicine, Clinical Center, National Institutes of Health, Bethesda, Maryland

Rodent models and genetically altered mice have recently become available to study many human diseases. A sensitive and accurate PET scanner for small animals would be useful to evaluate treatment of these diseases in rodent models. To examine the feasibility of performing quantitative PET studies, we performed dynamic scans with arterial blood sampling in anesthetized rats with the ATLAS (Advanced Technology Laboratory Animal Scanner) small animal PET scanner developed at the National Institutes of Health and ^{18}F-FDG and compared activities determined by PET scanning with those obtained by direct tissue sampling. **Methods:** Dynamic PET scans after a bolus of ~48 MBq (1.3 mCi) ^{18}F-FDG were performed in rats anesthetized with isoflurane. Arterial blood sampling was performed throughout the scanning period. At 60 min the rat was killed, and the brain was rapidly removed and dissected into 5 structures (thalamus [TH], cortex [CX], brain stem [BS], cerebellum [CB], and half brain). Activity in the tissue samples was compared with the mean activity of the last 5 min of calibrated PET data. **Results:** Plasma activity peaked at ~0.2 min and then cleared rapidly. Brain activity initially rose rapidly; the rate of increase then progressively slowed until activity was approximately constant between 30 and 60 min. Recovery coefficients (MBq/mL in PET images)/(MBq/mL in tissue samples) were 0.99 ± 0.04, 0.90 ± 0.19, 1.01 ± 0.24, 0.84 ± 0.05, and 1.01 ± 0.17, respectively, in TH, CX, BS, CB, and half brain (mean ± SD, n = 6–9). Cerebral glucose utilization determined by Patlak analyses of PET data measured 30–60 min after injection of ^{18}F-FDG was 31.7 ± 5.2, 23.9 ± 4.8, 29.9 ± 5.0, 39.3 ± 7.3, and 28.1 ± 4.6 μmol/100 g/min (mean ± SD, n = 9) in TH, CX, BS, CB, and whole brain, respectively. These results are consistent with a previous ^{14}C-deoxyglucose study of the isoflurane-anesthetized rat. **Conclusion:** Expected values for glucose metabolic rates and recovery coefficients near unity suggest that quantitatively accurate dynamic ^{18}F-FDG brain imaging can be performed in the rat with arterial blood sampling and the ATLAS small animal PET scanner.

Key Words: small animal imaging; ^{18}F-FDG; arterial blood sampling; dynamic scan; glucose utilization; brain

J Nucl Med 2004; 45:665–672

For >20 y, PET has been a powerful tool in imaging human subjects and now has numerous clinical applications in cardiology, oncology, and neurology. This technique allows quantitative in vivo determinations of the rates of various physiologic and biochemical processes, and it does so with minimal invasiveness. The spatial resolution of typical PET scanners used for humans, however, makes them unsuitable for brain studies in small animals. There are quantitative autoradiographic methods for use in small animals that have very fine spatial resolution, but these methods require killing the animal. Increasingly, rodent models and genetically altered mice are being developed to study human disease. Their cost, often-scant availability, and the desire to use them in longitudinal studies are all driving the development of quantitative imaging methods with better resolution suitable for repeated studies in small animals. In addition, there is a concerted effort to use fewer animals in experimental studies. Imaging the complete biodistribution rather than killing several animals for each time point not only reduces the number of animals but also has the added advantage that statistical comparisons of paired samples—

Received Sep. 10, 2003; revision accepted Dec. 8, 2003.

For correspondence contact: William C. Eckelman, PhD, Positron Emission Tomography Department, Building 10, Room 1C495, 10 Center Dr., MSC 1180, Bethesda, MD 20892.

E-mail: Eckelman@nih.gov

that is, the same animal before and after treatment—can be made, and this further reduces the number of animals needed. Small animal PET scanners have been developed (*1*) but maximizing detection sensitivity, spatial resolution, and resolution uniformity continue to remain a challenge.

Fully quantitative PET methods require not only accurate measurement of tissue activity but also a measure of the amount of radiotracer delivered to the tissue during the study interval, the so-called "input function." This represents a second challenge in small animal PET imaging. Sampling of arterial blood provides the most direct and appropriate measurement of the input function, although other less direct measures—such as sampling blood from other mice at specified time points and applying that to the experimental group (*2*), direct sampling of retroorbital blood from a mouse (*3*), blood sampling from the left ventricle plus PET scanning of the heart and liver of a mouse (*4*), and an automated microvolumetric blood sampler to draw the blood from the jugular vein in a mouse (*5*)—have been used. External measurements of blood activity—for example, from the left ventricle—cannot be used when radiolabeled species other than the parent compound are present in plasma, such as is the case with many receptor ligands, or when the radiotracer does not rapidly equilibrate between red blood cells and plasma to a known equilibrium distribution ratio. An alternative approach used in large animal PET scanning is to infer the input function through measurements in a reference tissue. Accurate determination of the activity in the reference tissue may be more difficult in small animals due to the relatively greater partial-volume effects in small animal imaging. Arterial blood sampling, when feasible, remains the most direct and accurate means of measuring the input function.

In response to the challenge of developing a high-sensitivity, high-resolution small animal PET scanner, the Imaging Physics Laboratory of the Nuclear Medicine Department, Clinical Center, National Institutes of Health, constructed the Advanced Technology Laboratory Animal Scanner (ATLAS) (*6*). In the present study, we explored the feasibility of using the ATLAS scanner for fully quantitative PET studies in anesthetized rats with rapid dynamic scanning and arterial blood sampling. In a feasibility study, we chose the well-known radiotracer ^{18}F-FDG, which is used for determination of regional rates of glucose utilization in all areas of the brain. Measurements of tissue activities determined with the ATLAS scanner were validated by comparison with those obtained by direct counting of tissue samples dissected immediately after completion of PET scanning. To demonstrate the feasibility of using time-resolved tissue data, regional cerebral glucose utilization ($rCMR_{glu}$) was determined from the arterial plasma and brain tissue time–activity curves by the multiple-time graphical analysis method of Patlak et al. (*7*,*8*). Additionally, we have performed a postmortem static scan of an anesthetized animal and an awake animal, in both of which ^{18}F-FDG had been administered 45 min previously, to illustrate the effect of isoflurane anesthesia on tracer uptake because it is well known that volatile anesthetics affect cerebral glucose utilization (*9*).

MATERIALS AND METHODS

Chemicals

Chemicals were obtained from the following sources: halothane was from Halocarbon, and isoflurane (Forane) was from Baxter. Euthanasia solution was obtained from Schering-Plough Animal Health Corp. (Beuthanasia-D special). ^{18}F-FDG was synthesized by a previously reported method (*10*) that is routinely used in our facility.

System Characteristics of ATLAS Small Animal PET Scanner

All PET images shown in this article were obtained with the ATLAS scanner. ATLAS has an 11.8-cm ring diameter, an 8-cm aperture, a 6-cm effective transverse field of view, and a 2-cm axial field of view. The scanner consists of 18 "phoswich," or depth-of-interaction, detector modules surrounding the imaging volume. The spatial resolution of this system is 1.8-mm full width at half maximum (FWHM) in the central field of view with filtered backprojection reconstruction and better than 1.5-mm FWHM when 3-dimensional ordered-subset expectation maximization (3D OSEM) reconstruction is used with resolution recovery and exact positioning of the lines of response (*1*). Sensitivity is 1.8% using a window of 250–650 keV and 2.7% with a window of 100–650 keV (*6*).

For scanner activity calibration, a cylinder 3.1 cm in diameter by 7.5-cm long was used to simulate the rat head and upper torso. This cylinder was filled with ^{18}F in water, centered in the scanner aperture, and imaged. The radioactivity in the cylinder was determined by a dose calibrator, and this value was divided by the volume of the cylinder to give concentration. Given these data, a calibration factor (C) was determined that related image counts to tracer concentration in the animal:

$$C = \frac{(\text{phantom kBq/mL } [\mu\text{Ci/mL}])}{(\text{cps in a voxel/voxel volume in image})}.$$

Concentration can then be calculated for any new image by multiplying the counts per second (cps) in a given voxel of that image by the calibration factor C. This calibration factor was determined periodically and did not vary significantly with time.

Animal Preparation

Normal adult male Sprague–Dawley rats (220–268 g) were purchased from Charles River Laboratories and maintained in a climate-controlled room on a 12-h light:dark cycle with food and water available ad libitum. They were deprived of food but allowed free access to water for 16 h before surgical preparation for the experiments. All animal procedures were in strict accordance with the National Institutes of Health Guide for the Care and Use of Laboratory Animals and approved by the Clinical Center Animal Care and Use Committee. Animals were anesthetized with halothane (5% induction and 1%–1.5% for maintenance in 30% O_2/70% N_2O). Polyethylene catheters (PE 50; Clay Adams) were inserted into left and right femoral arteries and the left femoral vein. One arterial catheter was used for continuous monitoring of mean arterial blood pressure (MABP) and the other was used for sampling of arterial blood. The length of the catheter used for

blood sampling was fixed precisely at 16 cm to minimize sampling errors due to catheter delay and dispersion. The venous catheter was used for injection of ^{18}F-FDG. The catheters were buried under the skin in a tunnel that was passed from the femoral area to the area behind the neck, and the tips of the catheters were located under the skin in the area behind the neck. This placement of the catheters allows the animal to move freely without damaging the catheters. After the catheterizations, surgical wounds were treated with 5% lidocaine ointment and sutured. Duration of anesthesia during the surgical preparation was usually about 30 min. Throughout the surgical preparations and the experimental periods, body temperature was monitored by a rectal probe and maintained at 37°C by a thermostatically controlled heating lamp (model 73 A; Yellow Springs Instrument Co., Inc.). At least 3 h were allowed for recovery from the surgery and anesthesia before the PET study. The surgical procedures were successful in >90% of the studies.

Physiologic Variables

In 4 animals, MABP was monitored continuously with a Micro-Med Blood Pressure Analyzer (model 300; Micro-Med) that had been calibrated with an air-damped mercury manometer. In all animals, arterial blood partial pressure of CO_2 (P_{CO_2}), partial pressure of O_2 (P_{O_2}), and pH were measured with a blood-gas analyzer (model 288 Blood Gas System; Ciba-Corning Diagnostics Corp.). Hematocrit was determined in arterial blood samples centrifuged in a Microfuge B (Beckman Instruments). Arterial plasma glucose concentration was determined with a Beckman Glucose Analyzer 2 (Beckman Instruments). Physiologic variables other than MABP were measured immediately before injection of the radiotracer and again approximately 35 min later.

PET Study

PET scans were performed in 9 rats. After at least 3-h recovery from catheterization surgery, the rat was reanesthetized with isoflurane (5% for induction and 2% for maintenance in 100% O_2) using a nose cone. The tunneling of the catheters was undone so that the catheters were readily accessible. After ~15-min preparation, the rat was placed in a prone position on the platform of the scanner. With the help of a laser beam attached to the scanner, the rat was positioned so that the center of the field of view was 12 mm caudal to the line between the lateral edges of the eyes. ^{18}F-FDG (49.9 ± 10.5 MBq [1.348 ± 0.284 mCi]; range, 37–62.9 MBq [1.0–1.7 mCi]; 300–700 μL in volume) was administered via the venous catheter over a period of about 15 s, and the catheter was immediately flushed with 100 μL of saline from a syringe connected with a custom-made Y-connector. Scanning was initiated at the onset of ^{18}F-FDG administration. A sequence of one hundred twenty 30-s images was acquired; total scanning time was 60 min. After the last scan, the rat was killed with a bolus venous injection of euthanasia solution.

To obtain a high-quality image and to visualize the effects of 2% isoflurane anesthesia on the uptake of ^{18}F-FDG, we conducted an ex vivo static scan of the head for 60 min on one rat who was awake and one rat who was anesthetized during the 45-min uptake period of ~63 MBq (1.7mCi) ^{18}F-FDG.

Arterial Blood Sampling

To determine the plasma time–activity curve, the blood sampling schedule of the quantitative autoradiographic 2-deoxy-D-^{14}C-glucose (2-^{14}C-DG) method (*9*) was followed—that is, 6 continuous samples over ~15 s and 13 additional blood samples taken at progressively increasing intervals (0.5, 0.75, 1, 2, 3, 5, 7.5, 10, 15, 25, 35, 45, 60 min). Blood samples, approximately 100 μL in volume, were withdrawn into polyethylene microcentrifuge tubes coated with heparin-lithium-fluoride (Beckman Instruments, Inc.), plasma was separated from red blood cells by centrifugation, and 40 μL of plasma were counted in a γ-counter (Wizard model 1480; PerkinElmer Life Sciences Inc.). The remaining plasma was used for the measurement of glucose concentration. To minimize blood loss, all dead-space volumes of blood collected in the sampling process were reinjected intravenously into the animal.

Direct Tissue Counting

Immediately after the rat was euthanized, the brain was taken out and separated into 2 parts, each including one hemisphere and half of the CB and BS. One part was weighed and counted; its concentration of radioactivity was used to calculate the whole brain radioactivity. From the other part, 4 structures were dissected (thalamus [TH], cortex [CX], cerebellum [CB], and brain stem [BS]), weighed, and counted in a γ-counter. All activities were expressed in MBq/mL, assuming the specific gravity of tissue to be 1.

Analysis of PET Data

Data from the scanner were formatted into 27 time frames (8 × 30 s, 6 × 60 s, 5 × 120 s, and 8 × 300 s). Images were reconstructed by 3D OSEM (*11*). No correction was made for attenuation or scatter. Counts detected by the scanner were converted into MBq/mL by use of a cross-calibration factor (325.63 scanner cps/mL per MBq/mL [0.01205 scanner cps/mL per nCi/mL]) previously determined in a phantom study. Additionally, one image containing the sum of all counts collected over the full 60-min interval was constructed for placement of regions of interest (ROIs). Due to its relatively low spatial resolution, ROIs were placed on the summed image, not by use of landmarks in that image, but rather by identifying the 3D coordinates of each structure in a rat brain atlas (*12*) and locating the approximate corresponding position in the PET image. TH, CX, and whole brain ROIs were drawn on coronal sections; the first coronal slice was 4 mm caudal from the tip of the frontal lobe. Each slice was 1.125-mm thick. CB and BS ROIs were placed on sagittal sections. ROIs were then transferred to the image for each time frame of data, and weighted average tissue activity was computed. A background ROI was also drawn outside the brain region. In all cases, the apparent activity in this region was very small during the course of a study and reflected the small contributions from random coincidence events and from scatter. Tissue time–activity curves were constructed by subtracting background activity from activity measured in each structure. Background-corrected tissue activity in the last frame of data (55–60 min after injection) was used for comparison with the directly counted tissue samples.

To verify the reproducibility of the ROI placement, 2 different readers separately drew the ROIs on the same regions of each animal and the results were compared. The interreader variability was 4.6% at its maximum with a SD of 3.4%. In addition, both readers redrew the ROIs after 1 mo or more from the first reading and again the results were compared. Reader 1 intravariability was 2.1% at its maximum value with a SD of 4.3% and reader 2 intravariability was 0.23% ± 0.73%.

Determination of $rCMR_{glu}$

The multiple-time graphical analysis technique of Patlak et al. (*7*,*8*) was used to calculate $rCMR_{glu}$. This technique requires that the normalized plasma activity ($\theta(T) = \int_0^T C_p^*(t)dt/C_p^*(T)$, where

$C_p^*(t)$ is the arterial plasma concentration of ^{18}F-FDG) be plotted on the abscissa and the normalized tissue activity ($C_i^*(T)/C_p^*(T)$, where $C_i^*(T)$ is the tissue activity) be plotted on the ordinate. After the ^{18}F-FDG in the tissue pool has equilibrated with that in the plasma, the graph becomes a straight line with slope K equal to the rate constant for net uptake and metabolism of ^{18}F-FDG in the brain. In this study, the 6 frames of data acquired in the interval 30–60 min were used to estimate K. $rCMR_{glu}$ was then calculated from the following equation:

$$rCMR_{glu} = KC_p/LC,$$

where C_p is the arterial plasma glucose concentration and LC is the lumped constant of the method (*9*). As the LC for ^{18}F-FDG has not yet been determined by a direct analytic method in rats, we used the value of the LC for 2-^{14}C-DG—that is, 0.48 (*9*).

RESULTS

Physiologic Variables

Physiologic variables before and 35 min after injection of ^{18}F-FDG are shown in Table 1. The animals weighed 241 ± 18 g (mean ± SD, $n = 9$). MABP, monitored continuously throughout the scanning period, remained steady at 85–89 mm Hg, slightly below the normal range. The hematocrit decreased statistically significantly ($P < 0.001$; paired Student t test), and the plasma glucose concentration increased statistically significantly ($P < 0.01$; paired Student t test) during the scanning interval. There were no changes in any of the other physiologic variables.

PET Images

Figure 1 illustrates the widespread decreases in $rCMR_{glu}$ in the isoflurane-anesthetized animal compared with the animal that was awake during the period of ^{18}F-FDG uptake. This is consistent with previously reported decreases in $rCMR_{glu}$ in most brain regions of 30%–75% in isoflurane-anesthetized rats compared with awake controls (*13*). Figure 2 is an image of the average activity over the 60-min scanning interval for one animal in the study. ROIs were drawn on this image as described for determination of tissue time–activity curves.

Time–Activity Curves

Time–activity curves in a typical animal are shown in Figure 3. The left ordinate represents the tissue activity and the right ordinate represents the plasma activity. The plasma activity peaked at 0.17 min and then cleared rapidly. In the 5 brain structures examined (whole brain, CX, TH, CB, and BS), activity initially rose rapidly; the rate of increase then progressively slowed until activity was approximately constant between 30 and 60 min. Tissue activities in the different structures varied over a fairly narrow range; heterogeneity between the structures was expected to have been diminished compared with conscious animals due to the use of anesthesia in this study.

Comparison Between Direct Tissue Counting Versus PET Image Analysis

The results from direct counting of the tissue samples and the PET image were converted to MBq/mL and compared (Table 2). The values obtained from the PET images were divided with the directly counted tissue activity to provide an estimate of the recovery rate (PET image activity/tissue activity). The recovery rate in whole brain was 1.01 ± 0.17 ($r = 0.71$) (mean ± SD and correlation coefficient, $n = 6$). In TH, CX, BS, and CB, recovery rates were 0.99 ± 0.04 ($r = 0.99$), 0.90 ± 0.19 ($r = 0.73$), 1.01 ± 0.24 ($r = 0.43$), and 0.84 ± 0.05 ($r = 0.96$), respectively (mean ± SD, $n = 9$).

Glucose Utilization Analysis with Patlak Plot

Patlak plots from one animal are shown in Figure 4. In each graph the slope of the curve is proportional to $rCMR_{glu}$. Here the decreased heterogeneity is seen from the similar slopes of each structure's graph. $rCMR_{glu}$ determined by Patlak analysis over the interval 30–60 min after injection of ^{18}F-FDG was 31.7 ± 5.2, 23.9 ± 4.8, 29.9 ± 5.0, 39.3 ± 7.3, and 28.1 ± 4.6 μmol/100 g/min (mean ± SD, $n = 9$) in TH, CX, BS, CB, and whole brain, respectively.

DISCUSSION

To our knowledge, the present study is the first report of dynamic scanning in anesthetized rats with a small PET scanner while concurrently sampling arterial blood. The study was undertaken to examine the feasibility of performing fully quantitative dynamic PET studies in small animals. We used the high-resolution, high-sensitivity ATLAS small animal PET scanner developed at the National Institutes of Health and the well-characterized radiotracer ^{18}F-FDG. We

TABLE 1
Physiologic Variables

Injection of ^{18}F-FDG	MABP (mm Hg)	Body temperature (°C)	Hematocrit (%)	Plasma glucose concentration (mg/dL)	Blood gas analysis		
					pH	P_{CO_2} (mm Hg)	P_{O_2} (mm Hg)
Immediately before	89 ± 6	35.8 ± 1.1	44 ± 3	145 ± 23	7.30 ± 0.05	53 ± 6	368 ± 153
35 min after	86 ± 7	36.1 ± 1.2	41 ± 4*	165 ± 29†	7.28 ± 0.04	55 ± 8	362 ± 144

*$P < 0.001$ indicates statistically significantly different from baseline (Student t test).
†$P < 0.01$ indicates statistically significantly different from baseline (Student t test).
Values are mean ± SD ($n = 4$ for MABP; $n = 9$ for other parameters).

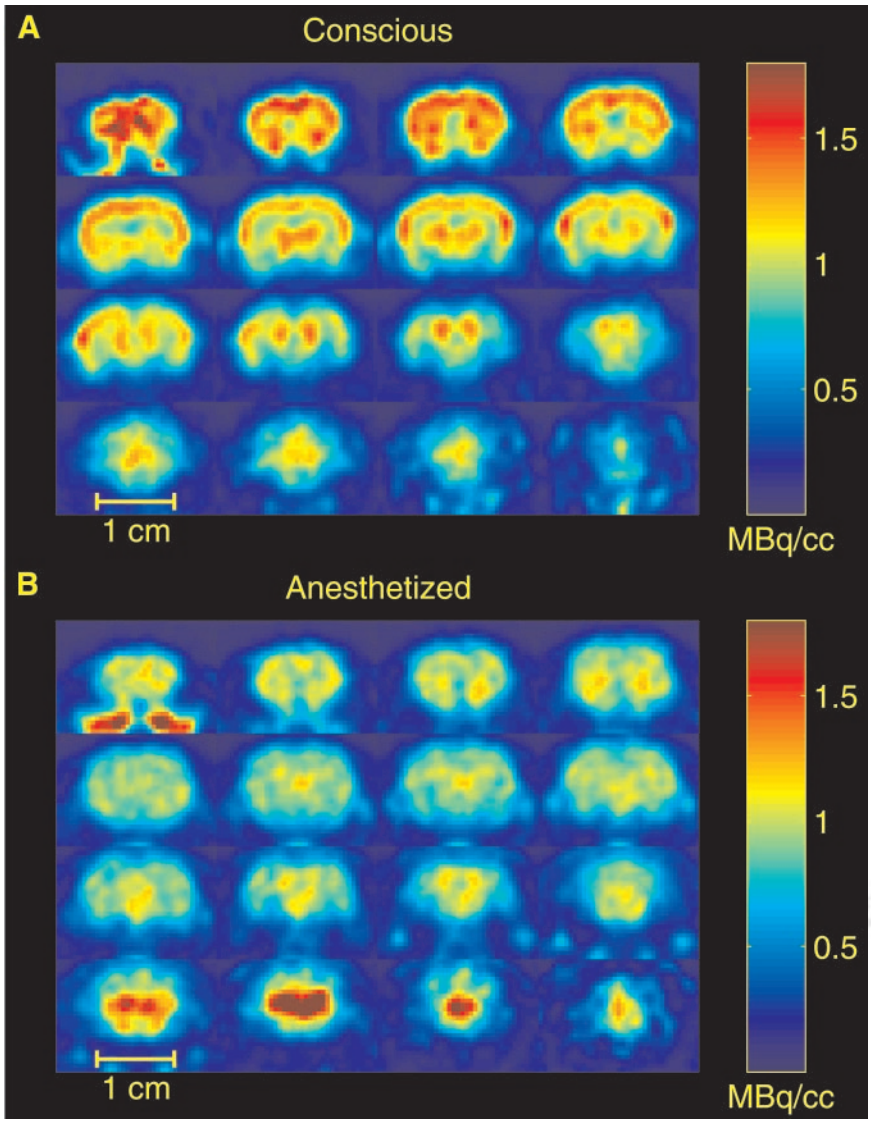

FIGURE 1. High-quality PET image of brain of rat that was awake (A) or under isoflurane anesthesia (B) during 45-min period of tracer uptake before scanning. After tracer uptake, animals were killed and were placed on scanner bed, and heads were scanned for 60-min interval. Note high cortical uptake of ^{18}F-FDG in awake animal that is much reduced in anesthetized rat. Compared with awake animal, brain uptake of ^{18}F-FDG is much less heterogeneous in anesthetized rat. Slice thickness is 1.125 mm. Injected doses were 63.9 and 64.8 MBq (1.73 and 1.75 mCi) in conscious and anesthetized rats, respectively.

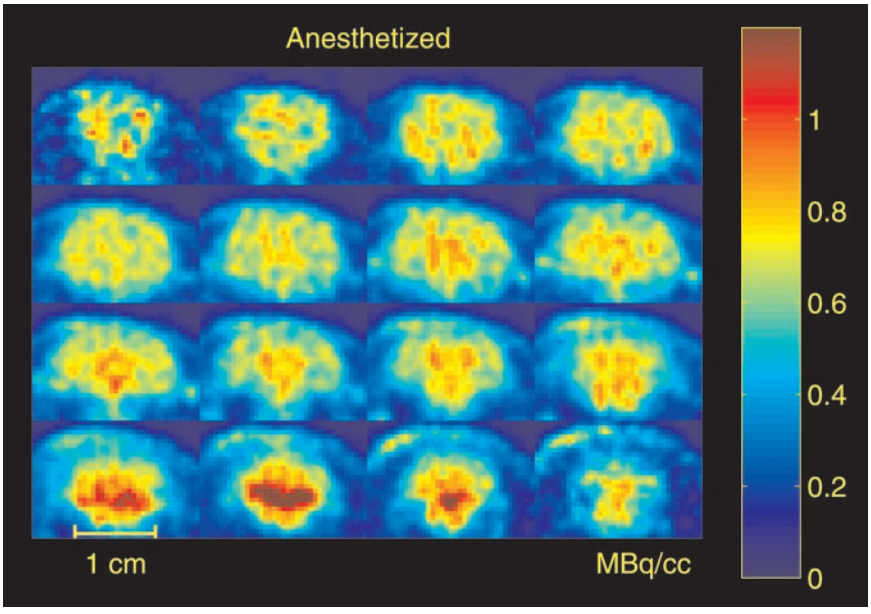

FIGURE 2. PET image of average activity during dynamic scanning of anesthetized rat from time of injection of ^{18}F-FDG until 60 min later. Sections are sliced coronally; first slice is 4 mm caudal from tip of frontal lobe. Thickness of each slice is 1.125 mm. Note low degree of regional differentiation due to effects of anesthesia; this necessitated use of an atlas of rat brain to identify structures by their spatial coordinates rather than through landmarks in PET image. Animal received 58 MBq (1.56 mCi) ^{18}F-FDG.

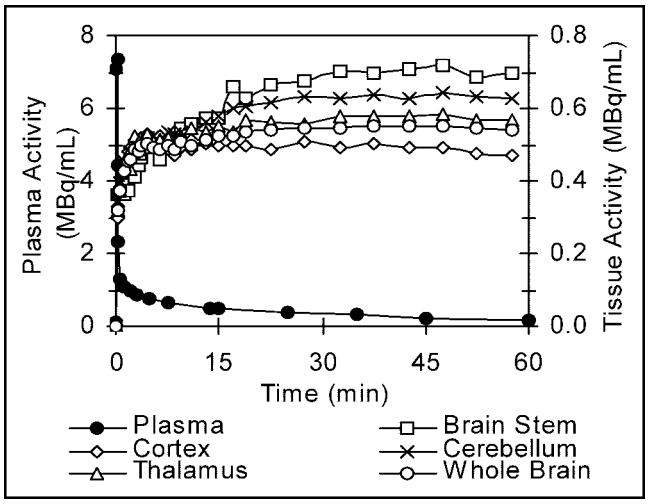

FIGURE 3. Time–activity curves of plasma (left ordinate) and whole brain, CX, TH, CB, and BS (right ordinate) from one animal. Plasma ^{18}F-FDG peaks at ~0.2 min and then clears rapidly. Tissue activities initially rise rapidly and then progressively less rapidly until they are approximately constant between 30 and 60 min. Due principally to effects of anesthesia, measured tissue activities exhibit a fairly narrow range, approximately 1.5 fold.

validated tissue measurements made with the PET scanner by comparison with γ-counting of ex vivo tissue samples and used the dynamic scans to determine tissue time–activity curves for determination of $rCMR_{glu}$.

Physiologic Variables

Rats in the present study had a MABP slightly lower than the normal range in unanesthetized animals, but within the range found in isoflurane-anesthetized rats (*13*). The decrease in the hematocrit was 7% from the 19 blood samples taken (total volume, 1.9 mL); although this was statistically significant, it probably did not have a great impact on the physiologic status of the animal because the animals were at rest and, therefore, did not require increased oxygen. In studies with radiotracers that can use whole blood for measuring the input function—that is, those that do not require separation of plasma—it may be possible to further reduce the blood sample volumes. Increases in plasma glucose concentration were moderate and may be due to the stress of blood loss. The plasma glucose concentration, however, remained within the normoglycemic range. pH was lower, P_{CO_2} was slightly higher, and P_{O_2} was higher than the normal limits in awake animals, consistent with effects usually seen under gas anesthetics.

PET Images

PET scanning in animals requires that the animal be immobilized; as there are currently no accepted alternatives for immobilization, all animals undergoing scanning must be anesthetized. In the present study we used isoflurane, which had profound effects on glucose utilization. To illustrate the differences in $rCMR_{glu}$ between the awake and isoflurane-anesthetized animal, we performed a postmortem, single scan of long duration on 2 additional animals: one awake during the period of uptake of ^{18}F-FDG and the other under isoflurane anesthesia during the uptake period. The effect of restraint on the biodistribution of ^{18}F-FDG in awake animals is unknown. The coronal images from these scans are shown in Figure 1. In the awake rat, there is the expected heterogeneity between the gray matter and the white matter. In the cortical area of the awake rat, the auditory CX has the highest uptake of ^{18}F-FDG (third and fourth slices in row 2). In contrast, the image of the anesthetized rat shows decreased activity and decreased hetero-

TABLE 2
Comparison Between Direct Tissue Counting and Activity Obtained from PET Images

Rat no.	Body weight (g)	Injected dose (MBq [mCi])	Recovery rate*				
			Whole brain	CX	TH	CB	BS
1	224	37.0 [1.000]	—	0.93	1.02	0.87	0.95
2	231	42.7 [1.153]	—	1.23	1.04	0.80	1.36
3	218	37.2 [1.006]	—	0.82	0.97	0.88	0.98
4	264	61.2 [1.655]	1.04	0.80	1.01	0.88	0.52
5	226	55.5 [1.501]	1.18	0.68	0.95	0.80	1.04
6	235	40.3 [1.090]	0.72	0.72	0.95	0.84	1.10
7	260	54.0 [1.460]	1.17	1.18	0.94	0.89	0.86
8	241	57.8 [1.563]	1.00	0.96	1.00	0.94	1.22
9	268	62.9 [1.700]	0.94	0.83	1.02	0.79	1.02
Mean ± SD	241 ± 18	49.9 ± 10.5 [1.348 ± 0.284]	1.01 ± 0.17	0.90 ± 0.19	0.99 ± 0.04	0.84 ± 0.05	1.01 ± 0.24
Correlation coefficient between direct tissue counting and activity obtained from PET images			0.71	0.73	0.99	0.96	0.43

*Recovery rate was determined as (activity in MBq/mL in PET image acquired 55–60 min after injection of ^{18}F-FDG)/(activity in dissected tissue in MBq/mL).

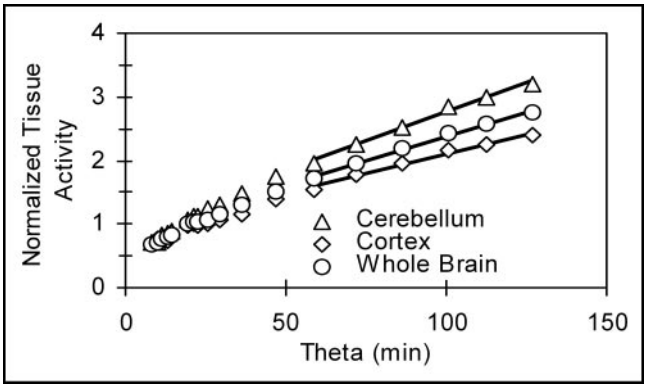

FIGURE 4. Patlak plot analysis of time–activity curves shown in Figure 3 for CB, CX, and whole brain. On abscissa is normalized plasma activity, $\theta(T) = \int_0^T C_p^*(t)dt/C_p^*(T)$, where $C_p^*(t)$ is arterial plasma concentration of ^{18}F-FDG. Tissue activity in each region divided by plasma activity is plotted on ordinate. After ^{18}F-FDG in tissue precursor pool(s) has equilibrated with ^{18}F-FDG in plasma, graph is a straight line with slope K proportional to rate of glucose utilization. Under anesthesia, glucose utilization is decreased and less heterogeneous than in awake animal; hence, slopes of graphs for regions fall into a fairly narrow range.

geneity in almost all regions. There is, however, an area that shows an increased uptake of ^{18}F-FDG compared with the awake rat (second slice, bottom row). This is in the area of the vestibular nucleus, but precise identification of the region needs to be determined with a method that has higher spatial resolution—for example, the quantitative autoradiographic 2-^{14}C-DG method. The effect of isoflurane anesthesia on $rCMR_{glu}$ in the vestibular nucleus is not presently known.

The loss of heterogeneity in the cortical area under isoflurane anesthesia is also evident in Figure 2, which shows activity in one animal integrated over the entire 60-min uptake interval of the dynamic PET acquisition. The integrated image also shows an area of very high uptake in the area of the vestibular nucleus. The less heterogeneous pattern of tracer uptake under isoflurane anesthesia is similar to that found with thiopental anesthesia (*9*) and reflects basal glucose metabolism. Even though ATLAS has better spatial resolution than previous-generation scanners (*14*), it is still difficult to determine detailed structures from the image. Therefore, in the present study, we outlined ROIs based on 3D coordinates from an atlas of the rat brain (*12*).

Time–Activity Curves

In the present study, we demonstrated the feasibility of performing arterial blood sampling during dynamic PET scans in rats by using the blood sampling techniques originally designed for use in the quantitative autoradiographic ^{14}C-deoxyglucose method. As illustrated in Figure 3, plasma radioactivity increased rapidly for ~0.2 min and then cleared rapidly, similar to the pattern that is observed after injection of 2-^{14}C-DG. The present study required 1.9 mL of blood to fully characterize the input function, and it is well understood that both the volume and the frequency of the samples must be reduced for measurements in mice. ^{14}C-Deoxyglucose studies in freely moving mice have demonstrated that glucose and ^{14}C-deoxyglucose concentrations can be measured in micro samples to reduce the total blood sampling volume to as little as 270 μL (*15*). The experience developed from these studies will be helpful for adapting PET methods for use in mice.

The time–activity curves in each of the tissues examined (whole brain, CX, TH, CB, and BS) were similar in shape. They initially rose rapidly, and then the rate of increase progressively slowed until activity was approximately constant between 30 and 60 min after injection of ^{18}F-FDG. The loss of heterogeneity is recognized in the time–activity curves from the fairly narrow range of tissue activities in the last frame of data: Activities ranged only approximately 1.5-fold. Although partial-volume effects due to the limited spatial resolution of the scanner contribute to the narrow range of activities, anesthesia plays a substantial role. In a previous quantitative ^{14}C-deoxyglucose study, the ratio of average gray matter to average white matter $rCMR_{glu}$ in isoflurane-anesthetized rats was 1.95:1, whereas the conscious animals exhibited a much greater range of activities with a ratio of 2.8:1 (*13*).

Comparison Between Direct Tissue Counting Versus PET Image Analysis

The whole brain, TH, and BS showed the best agreement between activities measured by PET and those measured by direct counting of the tissue samples. The whole brain was expected to give the best agreement due to lesser partial-volume effects. The TH is located in the center part of the brain, and, therefore, it had a higher degree of certainty in placing the ROI. The lower recovery rate in the CB may be due to difficulty in obtaining a clean dissection separating this structure from the adjacent region that has a very high uptake of ^{18}F-FDG, as shown in the PET images (Figs. 1 and 2). The decreased heterogeneity in the anesthesized rat brain may have reduced the partial-volume effects (*13*). Nevertheless, our data provide strong evidence that ATLAS can perform a dynamic ^{18}F-FDG scan because its data match well with the direct tissue counting.

CONCLUSION

The purpose of the present study was to examine the feasibility of the ATLAS small animal PET scanner to perform a dynamic scan with arterial blood sampling for measuring the input function. The results show that (a) physiologically it is possible to obtain 19 blood samples during 60 min for the time–activity curve of the blood and plasma without serious physiologic changes; (b) the direct tissue counting and the analyzed radioactivity of the images from the ATLAS small animal PET scanner are in good agreement; and (c) $rCMR_{glu}$, calculated by the multiple-time graphical analysis method of Patlak (*7,8*), is comparable to that in the previously reported study (*13*). Based on these

experiments, the ATLAS small animal PET scanner has the sensitivity and spatial resolution to perform a dynamic study in rat brain. The procedures described in this study can also be applied to quantitative studies for other radiotracers.

REFERENCES

1. Green MV, Seidel J, Vaquero JJ, Jagoda E, Lee I, Eckelman WC. High resolution PET, SPECT and projection imaging in small animals. *Comput Med Imaging Graph.* 2001;25:79–86.
2. Kallinowski F, Brownell AL, Vaupel P, Brownell GL. Combined tissue oxygen tension measurement and positron emission tomography studies on glucose utilization in oncogene-transformed cell line tumour xenografts in nude mice. *Br J Radiol.* 1991;64:350–359.
3. Hawkins RA, Choi Y, Scates S, et al. An animal model for in vivo evaluation of tumor glycolytic rates with positron emission tomography. *J Surg Oncol.* 1993; 53:104–109.
4. Green LA, Gamghir SS, Srinivasan A, et al. Noninvasive methods for quantitating blood time-activity curves from mouse PET images obtained with fluorine-18-fluorodeoxyglucose. *J Nucl Med.* 1998;39:729–734.
5. Lapointe D, Brasseur N, Cadorette J, et al. High-resolution PET imaging for in vivo monitoring of tumor response after photodynamic therapy in mice. *J Nucl Med.* 1999;40:876–882.
6. Seidel J, Vaquero JJ, Green MV. Resolution uniformity and sensitivity of the NIH ATLAS small animal PET scanner: comparison to simulated LSO scanners without depth-of-interaction capability. *IEEE Trans Nucl Sci.* 2003;50;1347–1350.
7. Patlak CS, Blasberg RG, Fenstermacher JD. Graphical evaluation of blood-to-brain transfer constants from multiple-time uptake data. *J Cereb Blood Flow Metab.* 1983;3:1–7.
8. Patlak CS, Blasberg RG. Graphical evaluation of blood-to-brain transfer constants from multiple-time uptake data: generalizations. *J Cereb Blood Flow Metab.* 1985;5:584–590.
9. Sokoloff L, Reivich M, Kennedy C, et al. The [^{14}C]deoxyglucose method for the measurement of local cerebral glucose utilization: theory, procedure, and normal values in the conscious and anesthetized albino rat. *J Neurochem.* 1977;28:897–916.
10. Adams HR, Channing MA, Divel JE, et al. Trend analysis of quality control data. In: Emran A, ed. *Chemists' Views of Imaging Centers.* New York, NY: Plenum Press; 1995:175–188.
11. Yao R, Seidel J, Johnson CA, Daube-Witherspoon ME, Green MV, Carson RE. Performance characteristics of the 3-D OSEM algorithm in the reconstruction of small animal PET images: ordered-subsets expectation-maximization. *IEEE Trans Med Imaging.* 2000;19:798–804.
12. Kruger L, Saprota S, Swanson L. *Photographic Atlas of the Rat Brain*. New York, NY: Cambridge University Press; 1995.
13. Maekawa T, Tommasino C, Shapiro HM, Keifer-Goodman J, Kohlenberger RW. Local cerebral blood flow and glucose utilization during isoflurane anesthesia in the rat. *Anesthesiology.* 1986;65:144–151.
14. Siegel S, Vaquero JJ, Aloj L, et al. Initial results from a PET/planar small animal imaging system. *IEEE Trans Nucl Sci.* 1999;46:571–575.
15. Jay TM, Jouvet M, des Rosiers MH. Local cerebral glucose utilization in the free moving mouse: a comparison during two stages of the activity-rest cycle. *Brain Res.* 1985;342:297–306.
16. Reivich M, Jehle J, Sokoloff L, Kety SS. Measurement of regional cerebral blood flow with antipyrine-^{14}C in awake cats. *J Appl Physiol.* 1969;27:296–300.
17. Cucchiara RF, Theye RA, Michenfelder JD. The effects of isoflurane on canine cerebral metabolism and blood flow. *Anesthesiology.* 1974;40:571–574.
18. Newberg LA, Milde JH, Michenfelder JD. The cerebral metabolic effects of isoflurane at and above concentrations that suppress cortical electrical activity. *Anesthesiology.* 1983;59:23–28.
19. Stullken EH Jr, Milde JH, Michenfelder JD, Tinker JH. The nonlinear responses of cerebral metabolism to low concentrations of halothane, enflurane, isoflurane, and thiopental. *Anesthesiology.* 1977;46:28–34.